The Cryosphere
Open Access
Discussions

Insights into ice stream dynamics through modeling their response to tidal forcing

S. H. R. Rosier[1,2], G. H. Gudmundsson[2], and J. A. M. Green[1]

[1]School of Ocean Sciences, Bangor University, Menai Bridge, LL59 5AB, UK
[2]British Antarctic Survey, High Cross, Madingley Rd., Cambridge, CB3 0ET, UK

Correspondence to: S. H. R. Rosier (s.rosier@bangor.ac.uk)

TCD

8, 659–689, 2014

3-D ice stream/shelf modeling of tidal interactions

S. H. R. Rosier et al.

Title Page

Abstract | Introduction

Conclusions | References

Tables | Figures

|◄ | ►|

◄ | ►

Back | Close

Full Screen / Esc

Printer-friendly Version

Interactive Discussion

Abstract

The tidal forcing of ice streams at their ocean boundary can serve as a natural experiment to gain an insight into their dynamics and constrain the basal sliding law. A 3-D visco-elastic full Stokes model of coupled ice-stream ice-shelf flow is used to investigate the response of ice streams to ocean tides. In agreement with previous results based on flow-line modeling and with a fixed grounding line position, we find that a non-linear basal sliding law can reproduce long period modulation of tidal forcing found in field observations, and the inclusions of lateral effects and grounding line migration do not alter this result. Further analysis of modeled ice stream flow shows a varying stress-coupling length scale of boundary effects upstream of the grounding line. We derive a visco-elastic stress coupling length scale from ice stream equations that depends on the forcing period and closely agrees with model output.

1 Introduction

The Antarctic Ice Sheet is surrounded by ocean and changes in this boundary forcing have important implications for its flow and future evolution. Ocean tides play an important role in ice dynamics of the continent; inducing currents that alter basal melting beneath the floating ice shelves (Makinson et al., 2011), affecting the motion of the ice shelves (Doake et al., 2002; Brunt et al., 2010; Makinson et al., 2012) and causing changes in short term and mean flow of ice streams, often far upstream of the grounding line (Anandakrishnan, 2003; Bindschadler and King, 2003; Bindschadler and Vornberger, 2003; Gudmundsson, 2006; Murray et al., 2007; Marsh et al., 2013).

Ice streams are regions of fast moving ice that form a link between the ice sheet and ice shelves, where most of the mass is lost from the continent, with implications for sea level rise (Vaughan, 2005; Alley et al., 2005; IPCC, 2007). In spite of the key role they play in ice mass loss from the Antarctic continent there are still many questions regarding the mechanisms controlling their flow.

The widespread use of GPS to measure ice stream flow has made available high temporal resolution data not previously possible with remote sensing techniques. The tidal signal in these measurements is easily distinguishable and can be used as a natural experiment to gain an insight into ice stream dynamics, in particular the nature of the basal sliding law (Gudmundsson, 2007, 2011; King et al., 2011; Walker et al., 2012). GPS observations of a strong tidal modulation of ice stream velocities at longer periods than the vertical ocean tidal forcing at the grounding line have raised questions about what mechanism could explain this and some of these theories are discussed in more detail below.

While previous studies have identified some key processes involved and demonstrated how the response is affected by basal conditions, all studies to date have been limited to flow-line situations, i.e. one horizontal dimension (1HD). It has thus not been possible to assess the effects in the transverse direction of the response of ice streams to tidal forcing. Given the importance of side drag in controlling the flow of ice streams this raises questions about the applicability of 1HD modeling studies. Here, we use a three dimensional model to address these open issues. We use a non-linear visco-elastic model with migrating grounding line to examine tidally induced perturbations in flow. In agreement with a previous 1HD study by Gudmundsson (2011) we find that a non-linear sliding law reproduces the general features of observations from the Rutford and other ice streams.

2 Overview of previous studies

Since the discovery of tidal effects on ice streams (Harrison, 1993; Anandakrishnan and Alley, 1997; Engelhardt and Kamb, 1998; Bindschadler and King, 2003; Bindschadler and Vornberger, 2003; Anandakrishnan, 2003) the interpretation and understanding of the mechanisms and impacts has continued to develop. Initial measurements of tidal forcing on ice were limited to the surface of the ice shelves (Williams and Robinson, 1980) and the hinging zone where ice flexure occurs near, near the ground-

ing line (Smith, 1991; Doake et al., 1987). In these regions tidal effects can be simply described with analytical solutions and elastic beam theory (Holdsworth, 1969, 1977; Reeh et al., 2003). Measurements made by Anandakrishnan and Alley (1997) on the Kamb Ice Stream first showed that these effects were not limited to regions within a few
5 ice thicknesses of the ocean boundary but could be transmitted far upstream.

The next step was the realisation that horizontal ice stream velocities could be modulated by the tides, much of the initial work focused on the Whillans Ice Stream (WIS) which was shown to exhibit a stick-slip behaviour resulting from vertical ocean tides (Anandakrishnan, 2003; Bindschadler and Vornberger, 2003; Bindschadler and King,
10 2003; Wiens et al., 2008; Winberry et al., 2009; Sergienko et al., 2009). This ice stream has mean annual speeds of greater than 300 m/a but the majority of motion occurs in brief bursts over time scales less than 1 h followed by longer periods where the ice is almost stationary. The Whillans Ice Plain portion of the WIS is dominated by stick-slip motion and the initiation of slip events strongly correlates with tides in the Ross sea as
15 accumulated stress is released.

Subsequently it was observed that ice streams can show a long period Msf response to a short period tidal forcing at both diurnal and semi-diurnal frequencies (Gudmundsson, 2006; Murray et al., 2007, Marsh et al., 2013). Of all the observed tidal effects on ice streams described above, it is arguably the long period modulation in horizontal
20 velocity, often far upstream of the grounding line, which has proven the most challenging to explain as it cannot be described by linear theory and requires a different mechanism.

One of the first attempts to explain the fortnightly variations in flow speed at Msf frequency observed on the Rutford Ice Stream was by Gudmundsson (2006, 2007)
25 who suggested that they arise due to the nonlinear relationship between basal motion and basal shear stress. Due to this nonlinearity, the increase in basal velocity arising from an increase in shear stress is larger than the decrease from an equal but opposite reduction in shear stress. As a result of this imbalance over one tidal cycle there is a net

forward motion and over several tidal cycles the variation in tidal range leads to long period modulation of flow speeds.

Murray et al. (2007) put forward a number of possible mechanisms, including Gudmundsson's model described above. They conclude that Gudmundsson's proposal cannot satisfactorily explain observations and a combination of processes are responsible. A partial ungrounding of the ice shelf from pinning points at high tides acts to increase velocity due to reduced basal resistive stress which is counteracted by increased back-stress exerted by the lifted ice shelf (Heinert and Riedel, 2007) leading to a complex relationship between tidal range and horizontal velocities at different frequencies. The authors argue that none of the current theories can completely reproduce the difference in response between the solstice and equinox. Subsequent work by King et al. (2010), using the same dataset, however showed that in fact the model presented by Gudmundsson (2007) could explain these observations and was consistent with a nonlinear sliding law with $m = 3$.

A study by Doake et al. (2002) of the Brunt Ice Shelf has also been cited to explain tidal response in ice streams (Murray et al., 2007; Aðalgeirsdóttir et al., 2008). Variations in basal friction from sub-ice ocean currents driven by the tides was proposed as a mechanism to induce lateral movement of the Ice Shelf at tidal frequencies and it was inferred that these motions would pull or push against the adjacent ice streams, thereby causing variations in horizontal velocities at the same frequency. Although this explanation for the motion of ice shelves has since been discounted (Makinson et al., 2012), the back stress arising from these motions will still affect the ice streams, but this cannot explain longer period frequencies which are not large in the ice shelf.

Another theory suggested by Aðalgeirsdóttir et al. (2008) is that basal melting near the grounding line, affecting subglacial pressure, might lead to some ice stream modulation at tidal frequencies as warmer water is transported to the grounding line by tidal currents. This idea seems unlikely to have any measurable impact on ice stream velocity however considering the typical magnitude of melting at daily or fortnightly time scales.

Full Screen / Esc

Printer-friendly Version

Interactive Discussion

Gudmundsson (2007) first proposed the link to a nonlinear basal sliding law and initial modelling efforts confirmed that a simple conceptual model including this process with $m = 3$ in the sliding law could produce the observed fortnightly variations in horizontal velocity. An extension of this work, in which ice was modelled as a non-linear visco-elastic medium and including all components of the equilibrium equation, further strengthened the argument (Gudmundsson, 2011). Work by King et al. (2011) showed that the same mechanism can reproduce ice stream velocity fluctuations from 4 h to 183 days observed in longer data series. A modeling study of the Bindschadler Ice Stream, forced primarily by diurnal rather than semidiurnal tidal constituents, further confirmed that a stress exponent $m > 1$ is needed but found that a value of 15 provided a better fit to the observed velocities (Walker et al., 2012). Some of the differences may be due to different model assumptions, for example the modeling study by Walker et al. (2012) solved a reduced set of equilibrium equations not including flexure stresses. According to the model by Gudmundsson (2011), flexure stresses can contribute to the tidal modulation in flow.

While the numerical flow-line study by Gudmundsson (2011) was capable of reproducing the key features observed in the data there were a number of processes ignored which weakens the argument, primarily the lack of transverse effects and a fixed grounding line position. In this paper we aim to address these issues with a full 3-D model including grounding line migration and show that a non-linear basal sliding law can fully explain observed long period modulations in flow.

3   Methods

The ice-stream/ice-shelf model is based around a commercial full stokes finite element analysis software MSC.Marc (MARC, 2013). While most of the results shown are for a fully 3-D model setup, simulations of a migrating grounding line were limited to a 2-D flow-line model due to computational limitations. An overview of the two model setups is shown in Fig. 1, where panels a and b are schematics of 2-D and 3-D models re-

spectively and panels c and d show the finite element grids. The field equations are the conservation of mass, linear momentum and angular momentum:

$$\frac{\text{D}\rho}{\text{D}t} + \rho v_{q,q} = 0 \qquad (1)$$

$$\sigma_{ij,j} + f_i = 0 \qquad (2)$$

$$\sigma_{ij} - \sigma_{ji} = 0 \qquad (3)$$

where $\text{D}/\text{D}t$ is the material time derivative, v_i are the components of the velocity vector, $\sigma_{i,j}$ are the components of the Cauchy stress tensor and f_i are the components of the gravity force per volume.

The rheological model is the same as that used by Gudmundsson (2011) and a more detailed description can be found there. Work by Reeh et al. (2003) showed that linear elastic models of ice were not adequate over tidal time scales and he proposed instead the use of a linear visco-elastic Burger's model of ice rheology. Following the arguments made in Gudmundsson (2011) we use a non-linear Maxwell model (consisting of a viscous damper and elastic spring connected in series) which has a close agreement to more complex Burger's model at the relevant time scales.

The Maxwell rheological model relates deviatoric stresses τ_{ij} and deviatoric strains e_{ij}:

$$\dot{e}_{ij} = \frac{1}{2G}\check{\tau}_{ij} + A\tau^{n-1}\tau_{ij}, \qquad (4)$$

where A is the rate factor, G is the shear modulus and $\check{\tau}$ denotes the upper-convected time derivative. The deviatoric stresses are defined as

$$\tau_{ij} = \sigma_{ij} - \frac{1}{3}\delta_{ij}\sigma_{pp} \qquad (5)$$

and the deviatoric strains as

$$e_{ij} = \epsilon_{ij} - \frac{1}{3}\delta_{ij}\epsilon_{pp} \qquad (6)$$

Title Page

Abstract | Introduction

Conclusions | References

Tables | Figures

◄ | ►

◄ | ►

Back | Close

Full Screen / Esc

Printer-friendly Version

Interactive Discussion

where σ_{ij} and ϵ_{ij} are the stresses and strains, respectively.

The model results presented here use a Young's modulus of between 1 to 3 GPa and a Poisson's ratio of 0.45. A number of runs were performed for a range of different values but it was found that the choice of values for these parameters did not affect the results qualitatively.

In the fully 3-D simulations, boundary conditions are applied which are not necessary for the 2-D case. Nodes on both the right and left hand boundaries of the model are clamped in the z direction, preventing ice from flowing out of the domain in this direction. In addition, the right hand boundary nodes are clamped in the x direction preventing any downstream flow. These additional boundary conditions produce a model with a clamped side wall to simulate an ice stream bounded by topography or ice with negligible velocity. The left hand boundary is treated as the ice stream medial line and in this way, although the model domain is only 32 km wide, the solution can be considered symmetrical and so the ice stream being modeled is in fact 64 km wide.

3.1 Contact

The contact option of MSC.Marc is used to simulate the detachment and migration of the grounding line. The ice and till layer are defined as separate deformable contact bodies such that during each incremental position the software checks whether every potential contact node from each body is near a contact segment. A contact segment is either an edge of a 2-D deformable body or the face of a 3-D deformable body. In order to maximise computational efficiency the software first defines a bounding box which quickly determines whether a node is near a segment, if the node falls within this box more sophisticated techniques are used to find the exact status of the node. A contact tolerance is defined for each surface and if a node is within this tolerance region it is considered to be in contact; if the node has passed through the tolerance range it is considered to have penetrated and a procedure is invoked to avoid this penetration.

Once two contact segments come into contact, a "glue" tying condition is applied so that there is no relative tangential motion between them. In the fully 3-D case this is

Title Page

Abstract | Introduction

Conclusions | References

Tables | Figures

◄ | ►►

◄ | ►

Back | Close

Full Screen / Esc

Printer-friendly Version

Interactive Discussion

as far as contact goes; the two contact bodies remain glued throughout the procedure and the ice flows primarily by deforming the till layer. For simulations in 2-D where the grounding line migrates the glue may separate, allowing the grounding line to move back and forth with the time varying ocean pressure. For the migration simulations presented here the glue separation criterion is simply that the two bodies are released when the tensile force between them exceeds a certain stress. In reality it would be expected that as soon as tensile forces are greater than 0, the ice would lift and the grounding line would migrate, however for numerical purposes the separation stress is defined as a very small number to stop numerical chattering between segments.

3.2 Basal boundary condition

Along the ice–bed interface upstream of the grounding line a Weertman sliding law is used of the form

$$\boldsymbol{v}_b = c|\mathbf{t}_b|^{m-1}\mathbf{t}_b, \tag{7}$$

where $\boldsymbol{v}_b$ is the basal sliding velocity, $\boldsymbol{t}_b$ is the basal traction

$$\boldsymbol{t}_b = \sigma\hat{\boldsymbol{n}} - (\hat{\boldsymbol{n}}^\mathsf{T} \cdot \sigma\hat{\boldsymbol{n}})\hat{\boldsymbol{n}} \tag{8}$$

and $\hat{\boldsymbol{n}}$ is a unit vector normal to the ice. The parameters c and m in Eq. (7) both have large effects on model results. c is referred to as basal slipperiness and reflects local conditions at the bed. This value is expected to change depending on the region of interest and in this study it is tuned to produce realistic surface velocities. The stress exponent m is the main focus of the modeling work presented here and previous modeling studies have used values ranging from 1 to infinity. Although the Weertman sliding law (first proposed by Weertman, 1957) has and continues to be used extensively in modeling basal motion of glaciers, and in spite of the importance that the stress exponent plays in modeling large scale ice masses, there is still debate as to its value.

3.3   Ice–ocean interface boundary condition

Along the ice–ocean interface beneath the ice shelf, downstream of the grounding line, water pressure p_w acts normal to the ice surface:

$$p_w = \rho_w g(S(t) - z), \tag{9}$$

5   where ρ_w is the water density, g is gravitational acceleration and S is the water surface. The tidal forcing in the model is introduced by making S an appropriate function of time with amplitude and period corresponding to the M_2 and S_2 tidal constituents. For the Siple Ice Coast the amplitudes and frequencies used were those of the O_1 and K_1 tidal constituents. The boundary condition is implemented as a linear elastic spring such 10   that the pressure normal to the ice is given by

$$p_w = k(z + z_0), \tag{10}$$

where k is the spring constant, z_0 the offset and z the position of the ice-ocean boundary. Substituting in $k = -\rho_w g$ and $z_0 = -S(t)$ gives Eq. (9). The result is that during high tide the maximum force is applied under the floating portion of the ice, lifting it 15   vertically by the same distance as the tidal amplitude except for around the hinging zone. The tidal force is multiplied by a factor which starts at 0, follows an arctangent function and asymptotes at 1 at around day 10 to avoid numerical issues with applying the full loading in one time-step.

At the upstream boundary of the model a pressure p is applied normal to the ice:

20   $$p = \rho_i g(s - z), \tag{11}$$

where s is the ice surface and ρ_i is the ice density which is assumed to be constant ($917\,\mathrm{kg\,m^{-3}}$).

At the downstream boundary of the model we assume the ice shelf terminates at a calving front and apply a normal pressure

25   $$p = \rho_w g(S - z), \tag{12}$$

Discussion Paper | Discussion Paper | Discussion Paper | Discussion Paper | Discussion Paper

for $z < 0$. For ice floating above water at the calving front $z > 0$ the boundary condition is simply $p = 0$. Although the assumption that the ice shelf is only 50 km long is out by an order of magnitude for many of the large ice streams outflowing from Antarctica it can be considered valid because the region of interest around and upstream of the grounding line is far enough away and fairly insensitive to the choice of boundary condition.

3.4 Element discretisation

In 2-D simulations an isoparametric, eight node quadrilateral element was used, optimized for plane strain applications. Biquadratic interpolation functions are used to represent coordinates and displacements and thus the strains have a linear variation within the element. The dimensions of the elements varied considerably from > 1 km along much of the ice shelf to 30 m around the grounding line. A grid refinement of 150 m was initially used around the grounding line but this was found to be insufficient and so the elements were subsequently reduced to the lower value quoted above. For full 3-D simulations an isoparametric, 20 node distorted brick was used with full integration, where each face consisted of 8 nodes with the same layout as the 2-D element described above. Dimensions vary considerably less than the 2-D geometry and are typically 1 km, 400 m and 2 km along the x, y and z planes, respectively.

4 Results

4.1 3-D Results

Numerical simulations initially focused on fully 3-D full stokes modeling of the response of an ice stream to tidal forcing. Figure 2 shows modeled horizontal displacements along the medial line of the ice stream 11, 21 and 31 km upstream of the grounding line. The tidal forcing consisted of M_2 and S_2 tidal constituents with amplitudes comparable

to those around the Rutford Ice Stream (RIS) and is plotted alongside the ice stream response (scaled down by a factor of 100 and shifted vertically).

The model geometry that produced these results had a domain as shown in Fig. 1, with ice thicknesses and slopes matching the average of those found on the RIS. As such the geometry does not exactly match that of the RIS, notably it does not vary laterally, but represents an idealised configuration which generally compares to those found on a typical ice stream. A stress exponent of $m = 3$ was used. Following the methods in previous studies, the basal slipperiness was changed in order to produce surface velocities of about $1\,\mathrm{m\,d^{-1}}$ (Gudmundsson, 2007, 2011; King et al., 2010; Walker et al., 2012).

The de-trended horizontal displacements in Fig. 2 show that the ice stream response, when forced with semi-diurnal tidal periods, is dominated by the Msf period (14.76 days). Furthermore, this effect becomes more pronounced higher upstream such that the semi-diurnal modulation of displacements disappears almost completely by 30 km upstream of the grounding line. These results match those of Gudmundsson (2011) and strengthen the hypothesis that the long period modulation of ice stream velocities is a result of a non-linear basal sliding law. The model was forced with a stress exponent of 1 and no long period effects occurred.

Figure 3 shows the results of a similar experiment which used a geometry and tidal forcing similar to those of the Siple Ice Coast ice streams rather than the RIS. The tide in this region is dominated by diurnal (K_1 and O_1) rather than semi-diurnal constituents and with lower amplitudes than around the RIS. This time the ice stream responds to diurnal forcing with Mf frequency modulation in horizontal de-trended displacements, however it does not dominate as strongly as the Msf did for semi-diurnal forcing. Note that the scale is different and the Mf signal 31 km upstream of the grounding line has an amplitude of only $\sim 1\,\mathrm{cm}$. This amplitude is too small to be measureable using current GPS techniques. We therefore conclude that Mf amplitudes on the Siple Ice Coast ice streams are expected to be small and difficult to measure, and about an order of magnitude less than the Msf signal found on the Filchner–Ronne ice streams.

4.2 2-D Results

In order to investigate the affect of a migrating grounding line on an ice stream's response to tidal forcing, a 2-D geometry was used with refinement near the grounding line as depicted in Fig. 1c. An initial control run used the same ice thickness and slopes as the 3-D case, but with a slightly smaller domain extending 80 km upstream and 40 km downstream of the grounding line respectively. In this initial simulation the two contact bodies were not allowed to separate and thus the grounding line would not migrate, as in the 3-D case. Since grounding line migration depends on the slope of the bed at the grounding line, with smaller slopes leading to larger migration distances, simulations with a migrating grounding line were done for various bed slopes and compared with the non migrating case. To keep other properties as similar as possible the slope was only changed in a region near the grounding line and the majority of the bed had the same slope as other simulations.

Results showing the comparison between different migrating cases and the fixed grounding line run are shown in Fig. 4. The uppermost curve is the semi-diurnal forcing scaled down and shifted vertically. Beneath this are four curves showing de-trended horizontal surface displacement 10 km upstream of the grounding line for the no breaking case and slopes ranging from $\gamma = 0.00375$ to 0.01. The final lowermost set of curves show the same but 30 km upstream. These results show that adding a migrating grounding line does not affect the main results demonstrated in this study and previous work and qualitatively the long period modulation is the same as for a non-migrating case. We find that runs with smaller slopes and hence larger migration distances produce a stronger Msf signal upstream of the grounding line, with the smallest slope producing displacements more than twice as large as in the fixed grounding line run.

4.3 Tidal analysis

A run using an identical model geometry and parameters as that shown in Fig. 2 was done but including values for all major tidal constituents (those with amplitudes greater

than 5 % of the M_2) around the RIS with amplitudes obtained from the CATS2008 tidal model (Padman et al., 2008). Subsequently, tidal analysis was done on these results using the t_tide MATLAB package (Pawlowicz et al., 2002). Figure 5 shows the calculated amplitude (Fig. 5a) and phase (Fig. 5b) of the Msf tidal constituent upstream of
5 the grounding line. The phase is almost constant apart from very close to the clamped side wall whereas amplitude decreases gradually and has not reached an apparent maximum even 30 km away from the boundary.

The model presented here provides an opportunity to investigate the effects of different forcing frequency on ice stream flow and stress transmission upstream of the
10 grounding line. Figure 6 shows the change in amplitude upstream of a grounding line for a simple sinusoidal boundary forcing with a range of frequencies. For these simulations the frequencies used at the boundary were not of a tidal nature, instead the ocean boundary was forced with a systematic spread of periods to get a clearer picture of the effect on an ice stream. In addition, ice rheology and the flow law were linearised
15 in order to make a comparison between our results and the expected response from simplified equations (see the discussion for more details). Amplitude is normalised and plotted on a log scale for clarity. Both amplitude and phase are shown to depend on the frequency of the forcing. In all cases the horizontal velocity amplitude response decays exponentially but at short forcing periods the rate of decay is a function of the period
20 while for longer forcing periods the curves converge to one solution. Runs were also done with a forcing period of 16 and 32 days but they have not been plotted here for the sake of clarity since they lie on top of the curve of $T = 12$.

5 Discussion

Previous modeling studies have successfully reproduced long period modulation of ice
25 stream flow by forcing their models with only semi-diurnal and diurnal tidal constituents and using a non-linear basal sliding law (Gudmundsson, 2007; King et al., 2010; Gudmundsson, 2011; Walker et al., 2012). This study demonstrates that including lateral

effects and grounding line migration do not alter this result and the effect on ice stream flow is qualitatively the same, confirming the hypothesis that a sliding law with $m > 1$ is required.

For an idealised geometry similar to that of the RIS the model produces a clear Msf frequency (Fig. 2) matching observations made in this area. When forcing the model with a geometry more typical of the Siple ice coast and diurnal tides the long period modulation remains but some features of the response are quite different (see Fig. 3). Firstly the long period response is at Mf frequency, as would be expected from a combination of K_1 and O_1 tidal constituents. In addition, the diurnal signal remains relatively strong even far upstream of the grounding line but the overall amplitudes for both long and short period motion are much smaller than the previous case. The amplitude of only ~ 1 cm is too small to be measureable using current GPS techniques. We therefore conclude that Mf amplitudes on the Siple Ice Coast ice streams are expected to be small and difficult to measure, and about an order of magnitude less than the Msf signal found on the Filchner–Ronne ice streams.

Simulations in which the grounding line could migrate back and forth with the tide give a long period modulation in flow that is qualitatively the same as those without migration (Fig. 4). Changing the slope of the bed near the grounding line in order to allow for more or less migration alters the magnitude of the Msf response only and the transmission of semi-diurnal forcing upstream appears to be unaffected.

Based on the results of the linearised model shown in Fig. 6 it is clear that the different responses at semi-diurnal, diurnal, Msf and Mf frequencies are expected. When the model is forced systematically with a range of different periods a clear relationship appears between the stress-coupling length scale of the signal amplitude upstream of the grounding line and the ocean boundary condition period. Deviations from the mean horizontal flow decay exponentially for periods of a few days. For longer periods this relationship breaks down and appears to be approaching a limit at $T = 12$ days. The cause of this lies in the visco-elastic rheology of the model; at short loading periods the ice behaves purely elastically but once this loading period passes a certain threshold

3-D ice stream/shelf modeling of tidal interactions

S. H. R. Rosier et al.

Title Page

Abstract | Introduction

Conclusions | References

Tables | Figures

|◄ | ►|

◄ | ►

Back | Close

Full Screen / Esc

Printer-friendly Version

Interactive Discussion

the ice is dominantly viscous, at which point loading period has no effect. We can relate this threshold to the effective relaxation time of the Maxwell model

$$\lambda = \frac{\eta}{G}; \tag{13}$$

where

$$\eta = \frac{\tau^{1-n}}{2A}. \tag{14}$$

Since $n = 1$ in these linearised runs this is easily solved and gives a time scale of 1.2 days which matches well with the model results described above.

It is also possible to estimate the expected stress-coupling length scale in order to compare it with our results. We follow a similar method to Walters (1989) who adds small variations in velocity to the SSA (Shallow Shelf Approximation) to derive a length scale, but carry this further by making velocity a function of period.

We can simplify the SSA for the linearised homogenous case as

$$4\partial_x(\eta h\partial_x u) - \frac{u}{c} = 0, \tag{15}$$

where h is ice thickness, c is bed slipperiness and u is ice velocity. The bed slipperiness is extracted from the model using the linearised Weertman sliding law (see Eq. 7 with $m = 1$ and where $\boldsymbol{t}_b$ and $\boldsymbol{v}_b$ are model outputs). Along with this equation we must make use of Eq. (4) which contains both the viscous and elastic components of deformation. Assuming η and h are not functions of x, adding a small periodic variation in the velocity of amplitude $\hat{u}$ such that

$$u = \overline{u} + \hat{u}e^{i(kx-\omega t)} \tag{16}$$

and substituting into Eq. (15), we can derive an expression for k:

$$k^2 = \frac{i\omega\lambda - 1}{4h\eta c}. \tag{17}$$

|◄ | ►|

◄ | ►

Back | Close

Full Screen / Esc

Printer-friendly Version

Interactive Discussion

where $\omega = \frac{2\pi}{T}$, T is the forcing period and λ is the relaxation time (Eq. 13). Since k^2 is a complex number that can be expressed as $\alpha + i\beta$ we find its roots to be $\pm(\gamma + \delta i)$ where

$$\gamma = \sqrt{\frac{-1 + \sqrt{1 + (\omega\lambda)^2}}{8hc\eta}} \tag{18}$$

and

$$\delta = \sqrt{\frac{1 + \sqrt{1 + (\omega\lambda)^2}}{8hc\eta}}. \tag{19}$$

Substituting the complex expression for k into Eq. (16) it becomes apparent that the velocity variation $\hat{u}$ has a decay part $e^{-\delta x}$ and a wave part $e^{i(\gamma x - \omega t)}$. The relevant length scale is therefore given by

$$L = \frac{1}{\delta} \tag{20}$$

and the phase velocity is

$$v_p = \frac{\omega}{\gamma}. \tag{21}$$

The length scale L determines how a perturbation in any of the field variables (i.e. velocity, strain, stress) decays with distance. This effect is due to transmission of stresses within the visco-elastic body, which in our model is instantaneous (in reality limited by the seismic velocity of ice and till). The length scale is, hence, not related to mass redistribution of ice with time that gives rise to a number of different length scales (e.g. Gudmundsson, 2003). Here we refer to L as the (visco-elastic) stress-coupling length scale.

Title Page

Abstract | Introduction

Conclusions | References

Tables | Figures

◄ | ►

◄ | ►

Back | Close

Full Screen / Esc

Printer-friendly Version

Interactive Discussion

By taking only the elastic or viscous contributions to the deviatoric strains in Eq. (4) it is possible to derive a length scale for a purely elastic or viscous material. The purely elastic length scale is

$$L_e = \sqrt{\frac{4hGcT}{\pi}} \tag{22}$$

and the purely viscous length scale is

$$L_v = \sqrt{4\eta hc}. \tag{23}$$

Crucially a time derivative only appears in the elastic contribution to deviatoric strain and it is from this that the stress-coupling length scale becomes a function of period, whereas for a purely viscous material there is no dependence on forcing period.

The two limiting cases appear in Eq. (19) such that as $\varpi \to 0$ (for very long periods) it simplifies to the purely viscous length scale and for $\varpi \gg 1$ the dependance on viscosity disappears to give the purely elastic length scale. The derivations of these stress-coupling length scales are simple for a Maxwell rheology because elastic and viscous strains can be related by $\varepsilon_{total} = \varepsilon_{viscous} + \varepsilon_{elastic}$.

A plot comparing forcing period with the three length scales calculated above along with the modeled length scale is shown in Fig. 7a. This shows that the modeled length scale agrees well with the elastic solution at short forcing periods, then deviates at longer periods approaching an asymptote for $T \gg \lambda$. The derived full visco-elastic solution provides a good fit with the modeled results. An analysis of stress-coupling length scale for the non-linear full 3-D model showed the same dependency on forcing period but since it cannot be compared directly with the results of the simple SSA solution it has not been included for the sake of brevity.

Walters (1989) fitted data from an Alaskan tide-water glacier on amplitude decay with distance from grounding line to a purely viscous version of the stress-coupling scale similar in form to Eq. (22). While the comparison made in that study provided a good agreement to observations the author effectively chooses a value of η that

works and since the decay is known to be exponential it is not unexpected that a good fit is obtained. Regardless, the same method cannot be used for forcing periods similar to or smaller than the Maxwell time scale. As has been shown, the stress-coupling length scale at these periods strongly depends on the period and either the purely elastic or full visco-elastic stress-coupling length scale should be used.

Phase velocities were calculated for each forcing period using a least squares fit and the results are compared with the analytical solution given by Eq. (21) in Fig. 7b. The phase velocities calculated from the model agree reasonably well with the analytical solution, although they appear to be slightly over-estimated particularly at short forcing periods. Some difference might be expected however since the equations have been derived from the SSA and the model is solving the full Stokes solution.

Previous studies cite a single value for the phase velocity of tidal forcing traveling upstream of an ice stream grounding line but these results show that phase velocity strongly depends on the forcing period up to a limit where $T \gg \lambda$. The semidiurnal tidal constituents have a period of 0.5 days and based on these results have a phase velocity of $1.45\,\text{m}\,\text{s}^{-1}$ whereas the longer period Mf and Msf constituents have a period of 14 days and would have a phase velocity of $0.27\,\text{m}\,\text{s}^{-1}$, over 5 times less. The range of values we find for phase velocity agree with the range of values typically found in the literature although, since most of these studies make it unclear how it has been calculated or which constituent they are considering, it is difficult to make a direct comparison.

6 Conclusions

The numerical model presented here finds that a non-linear sliding law with $m = 3$ produces long period modulation in ice stream flow, supporting the conclusions of previous work, and the inclusion of sidewalls and a migrating grounding line does not qualitatively change this result. Forcing the model with M_2 and S_2 tidal constituents reproduces the Msf surface velocity signal whereas a diurnal forcing of K_1 and O_1 gives

a different response with smaller long period modulation at Mf frequency, in both cases agreeing with GPS observations of ice streams subjected to these tidal forcings.

Upon closer inspection of model results we find a stress-coupling length scale that depends on the forcing period at timescales less than the Maxwell relaxation time. Comparing length scale obtained from the linearised model with the calculated length scales for a purely viscous or elastic response shows that the ice stream responds elastically at short forcing periods only (e.g. diurnal and semi-diurnal constituents). Once the forcing period is much larger than the relaxation time the stress-coupling length scale approaches that of a purely viscous medium (e.g. Msf and Mf consituents).

An ice stream's response to an external forcing is a function of the period of that forcing if the forcing period is short compared to the relaxation time. Ice streams are generally modeled as either viscous or elastic media. These results reflect that over short time scales an ice sheet behaves purely elastically and viscous effects can be neglected. Conversely when short term response can be ignored and changes are occuring over long time scales a purely viscous model may be suitable. Dependency on forcing period is an important consequence of an ice stream's visco-elastic rheology often missed by author's quoting only one value for measurements such as the propagation of stress upstream.

This study is limited in that, due to computational constraints, running the model in 3-D and allowing the grounding line to migrate at the same time was not feasible however these two effects can be considered separate and the combination of the two is not expected to change the results. In addition, the model geometry is an idealised form with a simple profile meaning the outputs cannot be directly compared to any one particular ice stream but must be considered as a generalised qualitative result.

We have further demonstrated how sensitive the response of ice streams to tides is on basal conditions. Despite here only focusing on the general qualitative aspects of available measurement, we are nevertheless able to confidently conclude that a linear sliding law is not consistent with observations. Although it may appear that we have not been able to constrain the form of the sliding law very tightly, and clearly much more

Title Page

Abstract   Introduction

Conclusions   References

Tables   Figures

◄   ►

◄   ►

Back   Close

Full Screen / Esc

Printer-friendly Version

Interactive Discussion

work remains to be done, we know of no other type of field observation or modeling work done to date that has allowed firm conclusions of this type to be made. This is despite decades spent in extracting information about basal control on motion by various other means. Currently, therefore the most successful and the most promising approach to study controls on basal motion is through modeling and measurements of tidally induced perturbation in flow.

References

Aðalgeirsdóttir, G., Smith, A. M., Murray, T., King, M. A., Makinson, K., Nicholls, K. W., and Behar, A. E.: Tidal influence on Rutford Ice Stream, West Antarctica: observations of surface flow and basal processes from closely spaced GPS and passive seismic stations, J. Glaciol., 54, 715–724, 2008. 663

Alley, R. B., Clark, P. U., Huybrechts, P., and Joughin, I.: Ice-sheet and sea-level changes, Science, 310, 456–60, 2005. 660

Anandakrishnan, S.: Ice stream D flow speed is strongly modulated by the tide beneath the Ross Ice Shelf, Geophys. Res. Lett., 30, 1361, doi:10.1029/2002GL016329, 2003. 660, 661, 662

Anandakrishnan, S. and Alley, R.: Tidal forcing of basal seismicity of ice stream C, West Antarctica, observed far inland, J. Geophys. Res., 102, 15183–15196, 1997. 661, 662

Bindschadler, R. and King, M. A.: Tidally controlled stick-slip discharge of a West Antarctic ice, Science, 301, 1087–1089, 2003. 660, 661, 662

Bindschadler, R. and Vornberger, P.: Tidally driven stickslip motion in the mouth of Whillans Ice Stream, Antarctica, Ann. Glaciol., 36, 263–272, 2003. 660, 661, 662

Brunt, K. M., King, M. A., Fricker, H. A., and Macayeal, D. R.: Flow of the Ross Ice Shelf, Antarctica, is modulated by the ocean tide, J. Glaciol., 56, 2005–2009, 2010. 660

3-D ice stream/shelf modeling of tidal interactions

S. H. R. Rosier et al.

Title Page

Abstract | Introduction

Conclusions | References

Tables | Figures

|◄ | ►|

◄ | ►

Back | Close

Full Screen / Esc

Printer-friendly Version

Interactive Discussion

Doake, C., Frolich, R., Mantripp, D., Smith, A., and Vaughan, D.: Glaciological studies on Rutford ice stream, Antarctica, J. Geophys. Res., 92, 8951–8960, 1987. 662

Doake, C. S. M., Corr, H. F. J., Nicholls, K. W., Gaffikin, A., Jenkins, A., Bertiger, W. I., and King, M. A.: Tide-induced lateral movement of Brunt Ice Shelf, Antarctica, Geophys. Res. Lett., 29, 1–4, 2002. 660, 663

Engelhardt, H. and Kamb, B.: Basal sliding of ice stream B, West Antarctica, J. Glaciol., 44, 223–230, 1998. 661

Gudmundsson, G. H.: Transmission of basal variability to a glacier surface, J. Geophys. Res.-Sol. Ea., 108, 2253, doi:10.1029/2002JB002107, 2003. 675

Gudmundsson, G. H.: Fortnightly variations in the flow velocity of Rutford Ice Stream, West Antarctica, Nature, 444, 1063–1064, 2006. 660, 662

Gudmundsson, G. H.: Tides and the flow of Rutford Ice Stream, West Antarctica, J. Geophys. Res., 112, F04007, doi:10.1029/2006JF000731, 2007. 661, 662, 663, 664, 670, 672

Gudmundsson, G. H.: Ice-stream response to ocean tides and the form of the basal sliding law, The Cryosphere, 5, 259–270, doi:10.5194/tc-5-259-2011, 2011. 661, 664, 665, 670, 672

Harrison, W.: Short-period observations of speed, strain and seismicity on Ice Stream B, Antarctica, J. Glaciol., 39, 463–470, 1993. 661

Heinert, M. and Riedel, B.: Parametric modelling of the geometrical ice–ocean interaction in the Ekstroemisen grounding zone based on short time-series, Geophys. J. Int., 169, 407–420, 2007. 663

Holdsworth, G.: Flexure of a floating ice tongue, J. Glaciol., 8, 133–397, 1969. 662

Holdsworth, G.: Tidal interaction with ice shelves, Ann. Geophys.-Italy, 33, 133–146, 1977. 662

IPCC: Climate Change 2007: The Physical Science Basis, Cambridge University Press, available at: http://www.worldcat.org/isbn/0521705967 (last access: 21 January 2014), 2007. 660

King, M. A., Murray, T., and Smith, A. M.: Non-linear responses of Rutford Ice Stream, Antarctica, to semi-diurnal and diurnal tidal forcing, J. Glaciol., 56, 167–176, 2010. 663, 670, 672

King, M. A., Makinson, K., and Gudmundsson, G. H.: Nonlinear interaction between ocean tides and the Larsen C Ice Shelf system, Geophys. Res. Lett., 38, 1–5, 2011. 661, 664

Makinson, K., Holland, P. R., Jenkins, A., Nicholls, K. W., and Holland, D. M.: Influence of tides on melting and freezing beneath Filchner–Ronne Ice Shelf, Antarctica, Geophys. Res. Lett., 38, L06601, doi:10.1029/2010GL046462, 2011. 660

Title Page

Abstract | Introduction

Conclusions | References

Tables | Figures

◄ | ►

◄ | ►

Back | Close

Full Screen / Esc

Printer-friendly Version

Interactive Discussion

Makinson, K., King, M. A., Nicholls, K. W., and Gudmundsson, G. H.: Diurnal and semidiurnal tide-induced lateral movement of Ronne Ice Shelf, Antarctica, Geophys. Res. Lett., 39, L10501, doi:10.1029/2012GL051636, 2012. 660, 663

MARC: Marc users manual, MSC Software Corporation, 2 MacArthur Place, Santa Ana, CA 92707, USA, 2013. 664

Marsh, O. J., Rack, W., Floricioiu, D., Golledge, N. R., and Lawson, W.: Tidally induced velocity variations of the Beardmore Glacier, Antarctica, and their representation in satellite measurements of ice velocity, The Cryosphere, 7, 1375–1384, doi:10.5194/tc-7-1375-2013, 2013. 660

Murray, T., Smith, A. M., King, M. A., and Weedon, G. P.: Ice flow modulated by tides at up to annual periods at Rutford Ice Stream, West Antarctica, Geophys. Res. Lett., 34, 6–11, 2007. 660, 663

Padman, L., Erofeeva, S. Y., and Fricker, H. A.: Improving Antarctic tide models by assimilation of ICESat laser altimetry over ice shelves, Geophys. Res. Lett., 35, L22504, doi:10.1029/2008GL035592, 2008. 672

Pawlowicz, R., Beardsley, B., and Lentz, S.: Classical tidal harmonic analysis including error estimates in MATLAB using T_TIDE, Comput. Geosci., 28, 929–937, 2002. 672

Reeh, N., Christensen, E. L., Mayer, C., and Olesen, O. B.: Tidal bending of glaciers: a linear viscoelastic approach, Ann. Glaciol., 37, 83–89, 2003. 662, 665

Sergienko, O. V., Macayeal, D. R., and Bindschadler, R.: Stick–slip behavior of ice streams: modeling investigations, Ann. Glaciol., 50, 87–94, 2009. 662

Smith, A.: The use of tiltmeters to study the dynamics of Antarctic ice-shelf grounding lines, J. Glaciol., 37, 51–58, 1991. 662

Vaughan, D.: How does the Antarctic ice sheet affect sea level rise?, Science, 308, 1877–1878, 2005. 660

Walker, R. T., Christianson, K., Parizek, B. R., Anandakrishnan, S., and Alley, R. B.: A viscoelastic flowline model applied to tidal forcing of Bindschadler Ice Stream, West Antarctica, Earth Planet. Sc. Lett., 319–320, 128–132, 2012. 661, 664, 670, 672

Walters, R. A.: Small-amplitude, short-period variations in the speed of a tide-water glacier in south-central alaska, USA, Ann. Glaciol., 12, 187–191, 1989. 674, 676

Weertman, J.: On the sliding of glaciers, J. Glaciol., 3, 33–38, 1957. 667

Wiens, D., Anandakrishnan, S., Winberry, J. P., and King, M. A.: Simultaneous teleseismic and geodetic observations of the stick–slip motion of an Antarctic ice stream, Nature, 453, 770–774, 2008. 662

Williams, R. and Robinson, E.: The ocean tide in the southern Ross Sea, J. Geophys. Res.-Oceans, 85, 6689–6696, 1980. 661

Winberry, J. P., Anandakrishnan, S., Alley, R. B., Bindschadler, R., and King, M. A.: Basal mechanics of ice streams: Insights from the stick–slip motion of Whillans Ice Stream, West Antarctica, J. Geophys. Res., 114, 1–11, 2009. 662

3-D ice stream/shelf modeling of tidal interactions

S. H. R. Rosier et al.

Title Page

Abstract	Introduction
Conclusions	References
Tables	Figures

|◀ | ▶|

◀ | ▶

Back | Close

Full Screen / Esc

Printer-friendly Version

Interactive Discussion

Title Page

Abstract | Introduction

Conclusions | References

Tables | Figures

|◄ | ►|

◄ | ►

Back | Close

Full Screen / Esc

Printer-friendly Version

Interactive Discussion
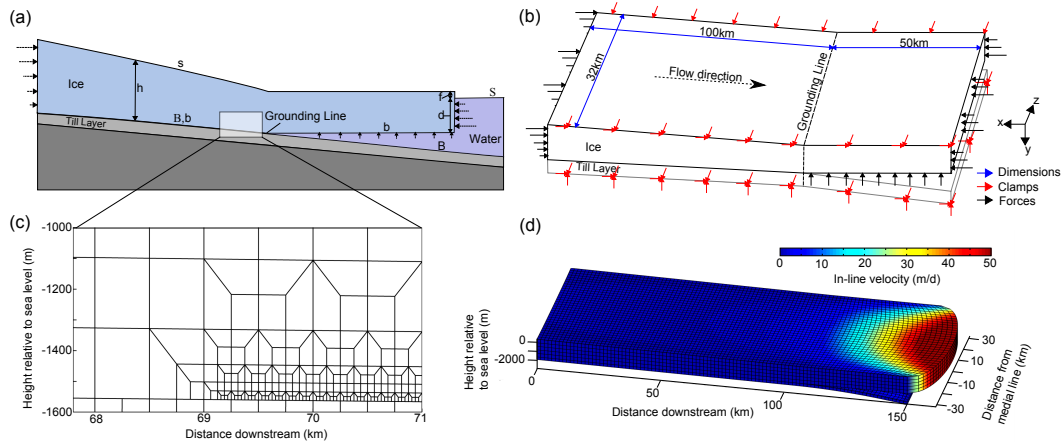
Fig. 1. Model setup for 2-D **(a, c)** and 3-D **(b, d)** simulations. **(a)** and **(b)** are schematic representations of the model domains while **(c)** and **(d)** show the model grid (**c** is zoomed in to show refinement near the grounding line). The 3-D grid in **(d)** has been vertically exaggerated by a factor of 4.
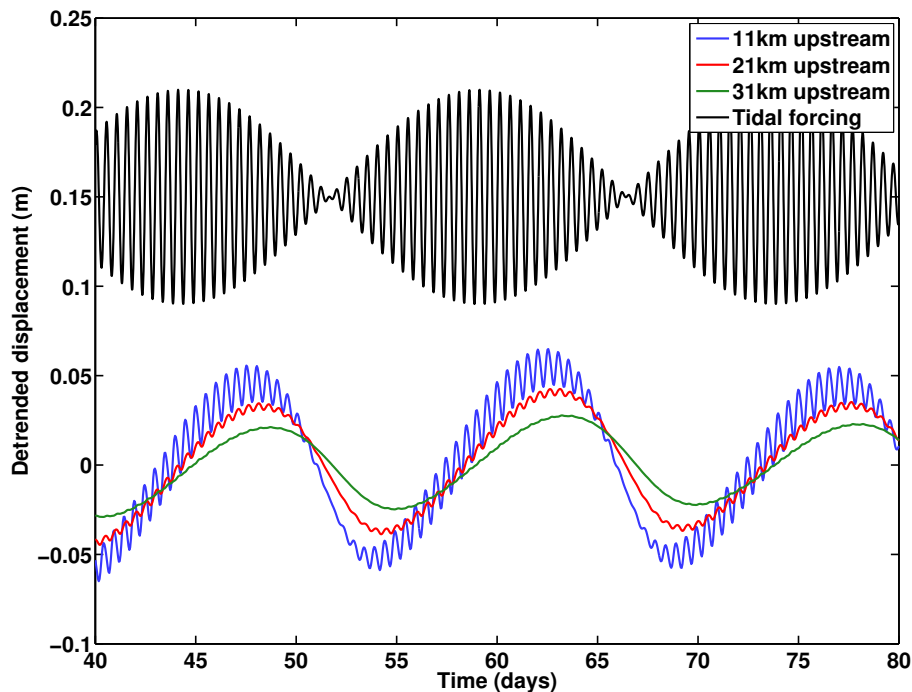
Fig. 2. De-trended in-line displacements at 11, 21 and 31 km upstream of the grounding line for the 3-D model run using an idealised Rutford Ice Stream geometry. The tidal forcing is also shown, scaled down by a factor of 100 and shifted vertically.
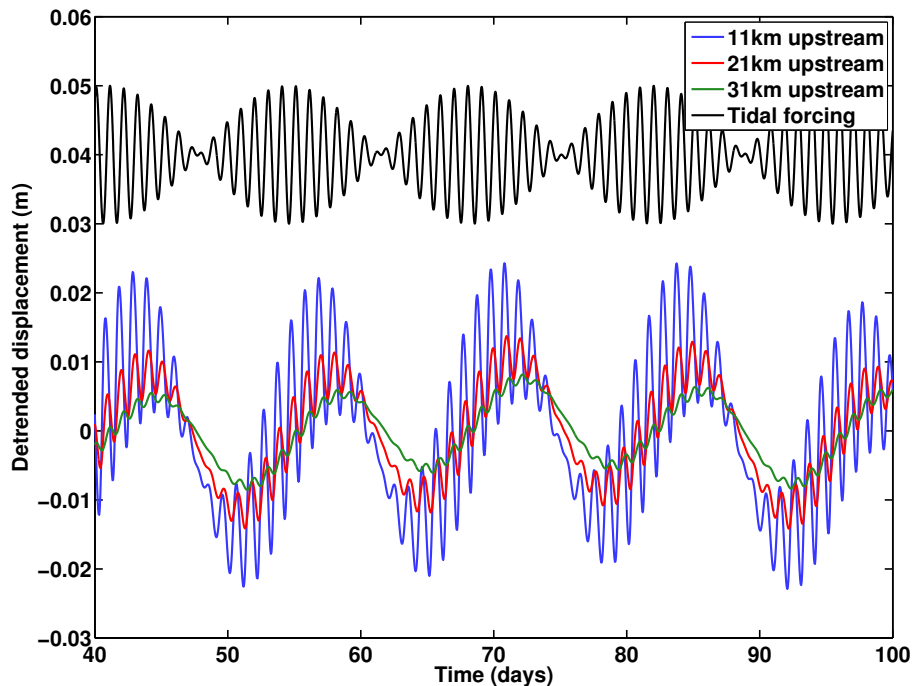
Fig. 3. De-trended in-line displacements at 11, 21 and 31 km upstream of the grounding line for the 3-D model run using an idealised Siple Ice Coast geometry. The tidal forcing is also shown, scaled down by a factor of 100 and shifted vertically.
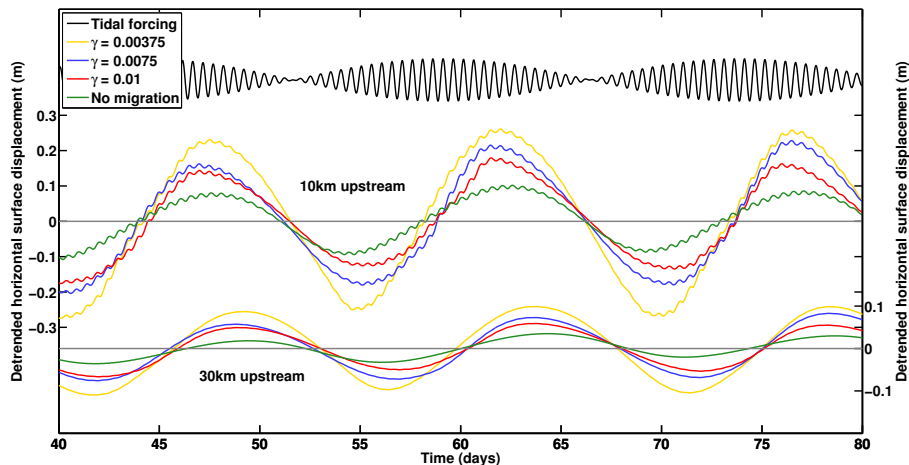
Fig. 4. Comparison of de-trended in-line displacements for geometries with different slopes. The upper plot shows the tidal forcing (scaled down by a factor of 100 and shifted vertically for clarity). The middle plot shows in line displacements 10 km upstream of the grounding line with and without migration and the lower plot shows the same 30 km upstream.

Full Screen / Esc

Printer-friendly Version

Interactive Discussion
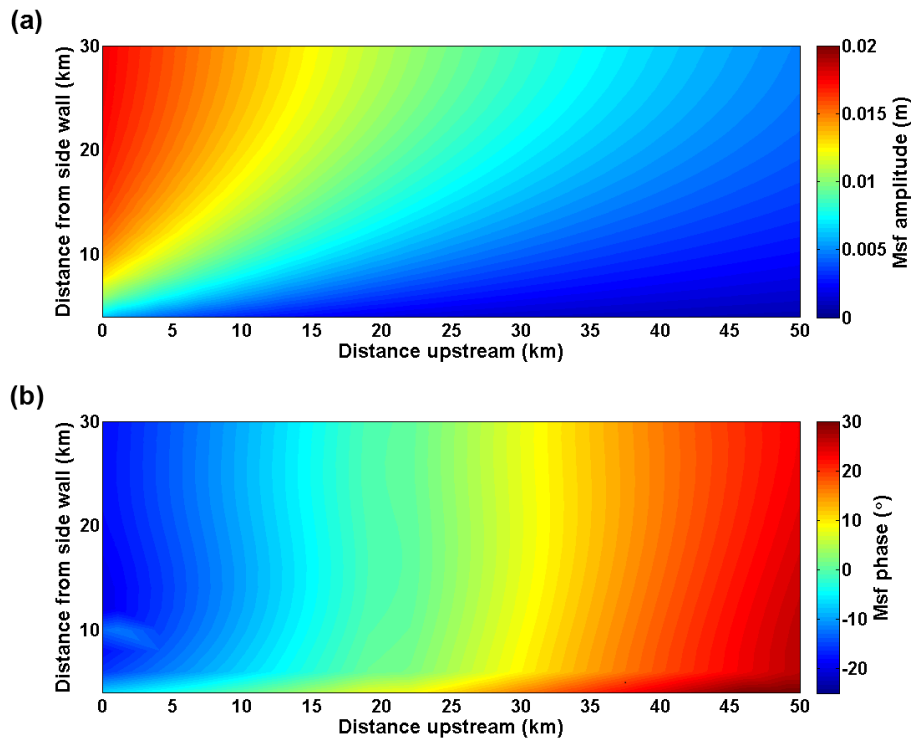
Fig. 5. Plots showing amplitude **(a)** and phase **(b)** of the Msf tidal constituent based on tidal analysis of de-trended horizontal surface displacement.
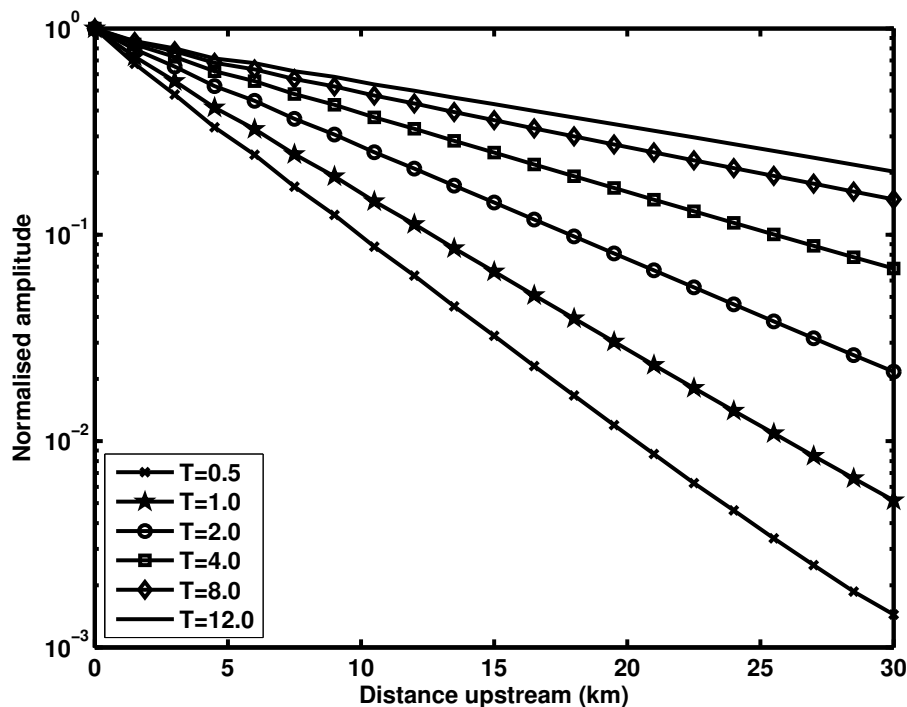
Fig. 6. Normalised amplitude response to various periods (in days) of boundary forcing as a function of distance upstream as calculated by the model. Model parameters used were: $A = 4.0^{-7}\,\mathrm{d^{-1}\,kPa^{-1}}$, $m = 1$, $n = 1$, $E = 3\,\mathrm{GPa}$, $\nu = 0.45$ and a value for the rate factor in the till to produce surface velocities of $1\,\mathrm{m\,d^{-1}}$. Note that amplitude is plotted on a log scale.
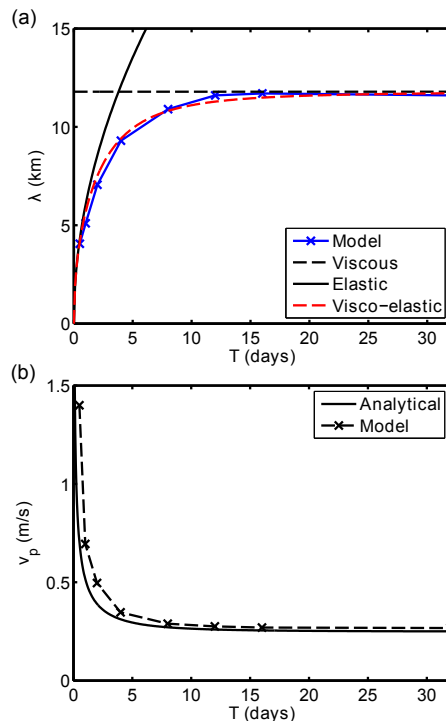
Fig. 7. Comparison of analytical solutions for stress-coupling length scale **(a)** and phase velocity **(b)** with model results. In **(a)** the solid and dashed black lines are the purely viscous and elastic length scales respectively as derived from the simplified SSA and the dashed red line is the combined visco-elastic response calculated from Eq. (20). The solid blue line is the modeled length scale calculated at loading periods marked with a cross. In **(b)** the phase velocity in the model (dashed line) was calculated by a least squares fit and compared to the analytical solution given in Eq. (21). Model parameters used were: $A = 4.0^{-7}\,\mathrm{d}^{-1}\,\mathrm{kPa}^{-1}$, $m = 1$, $n = 1$, $E = 3\,\mathrm{GPa}$, $v = 0.45$ and a value for the rate factor in the till to produce surface velocities of $1\,\mathrm{m\,d}^{-1}$.

Title Page

Abstract | Introduction

Conclusions | References

Tables | Figures

|◄ | ►|

◄ | ►

Back | Close

Full Screen / Esc

Printer-friendly Version

Interactive Discussion